



ISTITUTO NAZIONALE DI RICERCA METROLOGICA Repository Istituzionale

Condensed phase of Bose-Fermi mixtures with a pairing interaction

This is the author's submitted version of the contribution published as:

Original

Condensed phase of Bose-Fermi mixtures with a pairing interaction / Guidini, Andrea; Bertaina, Gianluca; Galli, Davide Emilio; Pieri, Pierbiagio. - In: PHYSICAL REVIEW A. - ISSN 1050-2947. - 91:2(2015), p. 3603. [10.1103/PhysRevA.91.023603]

Availability:

This version is available at: 11696/60807 since: 2021-03-04T18:45:44Z

Publisher:

American Physical Society

Published

DOI:10.1103/PhysRevA.91.023603

Terms of use:

This article is made available under terms and conditions as specified in the corresponding bibliographic description in the repository

Publisher copyright

American Physical Society (APS)

Copyright © American Physical Society (APS)

(Article begins on next page)

Condensed phase of Bose-Fermi mixtures with a pairing interaction

Andrea Guidini,¹ Gianluca Bertaina,² Davide Emilio Galli,² and Pierbiagio Pieri¹

¹*School of Science and Technology, Physics Division, University of Camerino,
Via Madonna delle Carceri 9, I-62032 Camerino, Italy*

²*Dipartimento di Fisica, Università degli Studi di Milano, Via Celoria 16, I-20133 Milano, Italy*
(Dated: May 18, 2018)

We study the condensed phase of a Bose-Fermi mixture with a tunable pairing interaction between bosons and fermions with many-body diagrammatic methods and fixed-node diffusion Quantum Monte Carlo simulations. A universal behavior of the condensate fraction and bosonic momentum distribution with respect to the boson concentration is found to hold in an extended range of boson-fermion couplings and concentrations. For vanishing boson density, we prove that the bosonic condensate fraction reduces to the quasiparticle weight Z of the Fermi polaron studied in the context of polarized Fermi gases, unifying in this way two apparently unrelated quantities.

PACS numbers: 03.75.Ss, 03.75.Hh, 32.30.Bv, 74.20.-z

Bose-Fermi (BF) mixtures with a tunable pairing interaction between bosons and fermions have been actively investigated in the context of ultra-cold gases [1–22], where the tunability of the BF interaction has been demonstrated and exploited in several experiments [23–32]. Previous work has shown that, even at zero temperature, a sufficiently strong BF attraction suppresses completely the boson condensate in mixtures where the number of bosons does not exceed the number of fermions [1, 12, 15]. This is due to pairing of bosons with fermions into molecules, which competes with condensation in momentum space. In particular, a first-order phase transition from a superfluid phase with a bosonic condensate, to a normal (molecular) phase without a condensate was recently demonstrated with fixed-node Diffusion Monte Carlo (FNDMC) simulations [19].

Here, we focus on the superfluid phase at zero temperature and present a many-body diagrammatic formalism able to describe this phase from weak to strong BF coupling. Our approach is validated by comparing it with previous [19] and new dedicated FNDMC calculations. By using both methods, we then analyze the condensate fraction and the momentum distributions, and establish a remarkable connection with the polaron problem in polarized Fermi gases.

Model and diagrammatic formalism - The system of our interest is a mixture of bosons of mass m_B and number density n_B , interacting with spinless fermions of mass m_F and number density n_F . The system is dilute, such that the range of all interactions can be considered smaller than the relevant inter-particle distances. The BF pairing interaction can be described then by an attractive contact potential, whose strength is parametrized in terms of the BF scattering length a_{BF} with the same regularization procedure commonly used for Fermi gases [33, 34]. The interaction between bosons is instead assumed to be repulsive, with scattering length a_{BB} of the order of the interaction range. No interaction between fermions is considered, since short-range interactions are suppressed by Pauli principle. We are interested in systems with concentration of bosons

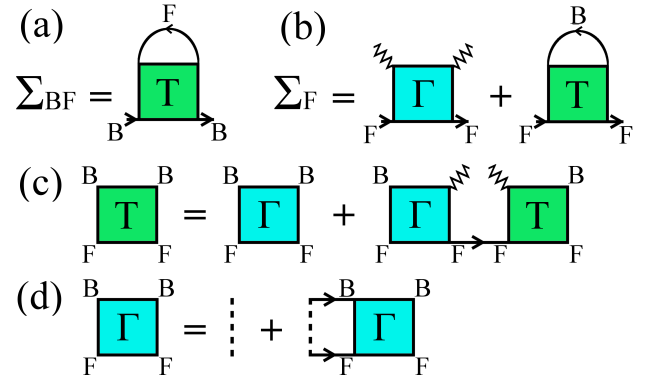


FIG. 1. Feynman's diagrams for Σ_{BF} , Σ_F , T , and Γ . Full lines correspond to bare boson (B) and fermion (F) Green's functions, dashed lines to bare BF interactions, zig-zag lines to condensate factors $\sqrt{n_0}$.

$x = n_B/n_F \leq 1$, where a full competition between pairing and condensation is allowed. A natural (inverse) length scale is then provided by the Fermi wave vector $k_F \equiv (6\pi^2 n_F)^{1/3}$, which can be combined with a_{BF} to define the dimensionless coupling strength $(k_F a_{BF})^{-1}$. For weak attraction a_{BF} is small and negative, such that $(k_F a_{BF})^{-1} \ll -1$ and perturbation theory is applicable [35, 36]. For strong attraction a_{BF} is small and positive, such that $(k_F a_{BF})^{-1} \gg 1$, and the system becomes effectively a mixture of molecules and unpaired fermions (if any), which can be described again by perturbation theory (now for a Fermi-Fermi mixture). The most challenging regime is then the intermediate one, where $|k_F a_{BF}| \gtrsim 1$ and perturbation theory fails.

Previous experience with the similar problem of the BCS-BEC crossover [37–40] suggests that selection of an appropriate class of diagrams might provide a reliable approach even in this non-perturbative regime. Let us consider first the boson component. In the absence of coupling with fermions, and for a boson gas parameter $\eta = n_B a_{BB}^3 \ll 1$, bosons can be described at $T = 0$ by Bogoliubov theory, corresponding to the

values $8\pi a_{\text{BB}}n_0/m_{\text{B}}$ and $4\pi a_{\text{BB}}n_0/m_{\text{B}}$ for the normal and anomalous self-energies, respectively (where n_0 is the condensate density and we set $\hbar = 1$ throughout). On the other hand, previous work for the *normal* phase shows that pairing correlations between bosons and fermions can be included rather accurately by a T-matrix type of self-energy [12, 16]. We extend this self-energy to the condensed phase by adding the contribution Σ_{BF} of Fig. 1(a) to the Bogoliubov contribution in the normal self-energy Σ_{B}^{11} . The many-body T-matrix (T) appearing in Σ_{BF} extends to the condensed phase the corresponding T-matrix (Γ) used in the normal phase [12, 16] by including condensate lines, as represented by the diagrams (c) and (d) of Fig. 1 [41]. We neglect here any diagram containing more than one T-matrix: pairing contributions are then excluded from the anomalous self-energy Σ_{B}^{12} . Feynman's rules for the finite temperature formalism then yield in the zero temperature limit:

$$\Sigma_{\text{B}}^{11}(\bar{k}) = \Sigma_{\text{BF}}(\bar{k}) + \frac{8\pi a_{\text{BB}}}{m_{\text{B}}}n_0 \quad (1)$$

$$\Sigma_{\text{B}}^{12}(\bar{k}) = \frac{4\pi a_{\text{BB}}}{m_{\text{B}}}n_0 \quad (2)$$

$$\Sigma_{\text{BF}}(\bar{k}) = \int \frac{d\mathbf{P}}{(2\pi)^3} \int \frac{d\Omega}{2\pi} \text{T}(\bar{P}) G_{\text{F}}^0(\bar{P} - \bar{k}), \quad (3)$$

where

$$\text{T}(\bar{P})^{-1} = \Gamma(\bar{P})^{-1} - n_0 G_{\text{F}}^0(\bar{P}) \quad (4)$$

$$\Gamma(\bar{P})^{-1} = \frac{m_{\text{r}}}{2\pi a_{\text{BF}}} - \frac{m_{\text{r}}^{\frac{3}{2}}}{\sqrt{2}\pi} \left[\frac{P^2}{2M} - 2\mu - i\Omega \right]^{\frac{1}{2}} - I_{\text{F}}(\bar{P}) \quad (5)$$

$$I_{\text{F}}(\bar{P}) \equiv \int \frac{d\mathbf{p}}{(2\pi)^3} \frac{\Theta(-\xi_{\mathbf{P}-\mathbf{p}}^{\text{F}})}{\xi_{\mathbf{P}-\mathbf{p}}^{\text{F}} + \xi_{\mathbf{P}}^{\text{B}} - i\Omega}. \quad (6)$$

In the above expressions we have introduced a 4-vector notation $\bar{P} \equiv (\mathbf{P}, i\Omega)$, $\bar{k} \equiv (\mathbf{k}, i\omega)$, where \mathbf{P}, \mathbf{k} are momenta and Ω, ω are frequencies. The bare Green's functions are given by $G_s^0(\bar{k})^{-1} = i\omega - \xi_{\mathbf{k}}^s$, where $\xi_{\mathbf{p}}^s = p^2/2m_s - \mu_s$ and $s = \text{B, F}$, while $\mu \equiv (\mu_{\text{B}} + \mu_{\text{F}})/2$ and $m_{\text{r}} = m_{\text{B}}m_{\text{F}}/(m_{\text{B}} + m_{\text{F}})$. A closed form expression for $I_{\text{F}}(\bar{P})$ is reported in [16].

The fermionic self-energy is due only to the coupling with bosons. In this case, the T-matrix can be closed in the diagram either with a boson propagator or with two condensate insertions. The second choice, however, produces in general *improper* self-energy diagrams, which would lead to a double-counting when inserted in the Dyson's equation for the dressed fermion Green's function. *Proper* diagrams are obtained by replacing T with Γ in this contribution, as shown in Fig. 1(b). The fermionic self-energy is then given by:

$$\Sigma_{\text{F}}(\bar{k}) = n_0 \Gamma(\bar{k}) - \int \frac{d\mathbf{P}}{(2\pi)^3} \int \frac{d\Omega}{2\pi} \text{T}(\bar{P}) G_{\text{B}}^0(\bar{P} - \bar{k}). \quad (7)$$

The self-energies (1), (2), and (7) determine the dressed boson and fermion Green's functions, once inserted in the

corresponding Dyson's equations:

$$G_{\text{B}}'(\bar{k})^{-1} = i\omega - \xi_{\mathbf{k}}^{\text{B}} - \Sigma_{\text{B}}^{11}(\bar{k}) + \frac{\Sigma_{\text{B}}^{12}(\bar{k})^2}{i\omega + \xi_{\mathbf{k}}^{\text{B}} + \Sigma_{\text{B}}^{11}(-\bar{k})} \quad (8)$$

and $G_{\text{F}}(\bar{k})^{-1} = G_{\text{F}}^0(\bar{k})^{-1} - \Sigma_{\text{F}}(\bar{k})$. The momentum distribution functions are in turn obtained by an integration over ω : $n_{\text{F}}(\mathbf{k}) = \int \frac{d\omega}{2\pi} G_{\text{F}}(\bar{k}) e^{i\omega 0^+}$ and $n_{\text{B}}(\mathbf{k}) = -\int \frac{d\omega}{2\pi} G_{\text{B}}'(\bar{k}) e^{i\omega 0^+}$ where $\mathbf{k} \neq 0$ for the bosons. A further integration over \mathbf{k} yields the fermion density $n_{\text{F}} = \int \frac{d\mathbf{k}}{(2\pi)^3} n_{\text{F}}(\mathbf{k})$ and the out-of-condensate density $n_{\text{B}}' = \int \frac{d\mathbf{k}}{(2\pi)^3} n_{\text{B}}(\mathbf{k})$, to which the condensate density n_0 must be added to get the boson density $n_{\text{B}} = n_0 + n_{\text{B}}'$. These T-matrix approximation (TMA) equations are finally supplemented by the Hugenholtz-Pines relation [43]: $\mu_{\text{B}} = \Sigma_{\text{B}}^{11}(0) - \Sigma_{\text{B}}^{12}(0)$, which, together with the above number equations, allows one to determine μ_{B} , μ_{F} , and n_0 for given values of n_{B} and n_{F} .

Quantum Monte Carlo (QMC) method - We estimate the momentum distributions also with the Variational Monte Carlo (VMC) and FNDMC methods, which stochastically solve the Schrödinger equation either with a variational wave function Ψ_T , or with an imaginary-time-projected wave function $\Psi_{\tau} = e^{-\tau \hat{H}} \Psi_T$, whose nodal surface is constrained to that of Ψ_T so to circumvent the fermionic sign problem [44]. We estimate $n_s(k)$ in VMC with $n_s^V(k) = \langle \Psi_T | \hat{n}_k | \Psi_T \rangle / \langle \Psi_T | \Psi_T \rangle$, where \hat{n}_k is the number operator in momentum space averaged over direction, while FNDMC provides the mixed estimator $n_s^M(k) = \lim_{\tau \rightarrow \infty} \langle \Psi_T | \hat{n}_k | \Psi_{\tau} \rangle / \langle \Psi_T | \Psi_{\tau} \rangle$. A common way to reduce the bias introduced by Ψ_T in the mixed estimator is to perform the extrapolations $n_s^{E1} = (n_s^M)^2 / n_s^V$ or $n_s^{E2} = 2n_s^M - n_s^V$, where the dependence on $\delta\Psi = \Psi_{\infty} - \Psi_T$ is second order. In practice, we use the differences between $n_s^{E1}(k)$ and $n_s^{E2}(k)$ as a systematic error on top of the statistical error. Simulations are carried out in a box of volume $L^3 = N_{\text{F}}/n_{\text{F}}$ with periodic boundary conditions, with a number of fermions up to $N_{\text{F}} = 57$ and a number of bosons N_{B} varying with x . Details of the model potentials are the same as in [19]. We use a trial wave function of the form $\Psi_T(\mathbf{R}) = J(\mathbf{R})\Phi(\mathbf{R})$, where $J(\mathbf{R}) = \prod_{\alpha,i} f_{\text{BF}}(r_{\alpha i}) \prod_{\alpha,\beta} f_{\text{BB}}(r_{\alpha\beta})$ is a Jastrow function of the fermionic (Latin) and bosonic (Greek) coordinates and Φ is a Slater determinant of plane waves for the fermions. At distances $r < \bar{R}_{ss'}$, the functions $f_{ss'}$ are determined by solving the relevant two-body problems. For $r > \bar{R}_{\text{BF}}$, $f_{\text{BF}}(r) = \exp[-u(r) - u(L-r) + 2u(L/2)]$ with $u(r) = c_0 + c_1/r + c_2/r^2$, where c_0 and c_1 are fixed by continuity at \bar{R}_{BF} , while \bar{R}_{BF} and c_2 are variational parameters to be optimized [45]. We set $\bar{R}_{\text{BB}} = L/2$.

Results - Figure 2(a) and (b) report the coupling dependence of μ_{B} and μ_{F} (normalized to the Fermi energy $E_{\text{F}} = k_{\text{F}}^2/2m_{\text{F}}$) as obtained by solving the TMA equations for $m_{\text{B}} = m_{\text{F}}$, $\eta = 3 \times 10^{-3}$, and three different values of x . The chemical potential μ_{B} tends to the mean-field value $4\pi a_{\text{BB}}n_0/m_{\text{B}}$ in the weak-coupling limit $(k_{\text{F}}a_{\text{BF}})^{-1} \ll -1$, while it approaches $-\epsilon_0$, where

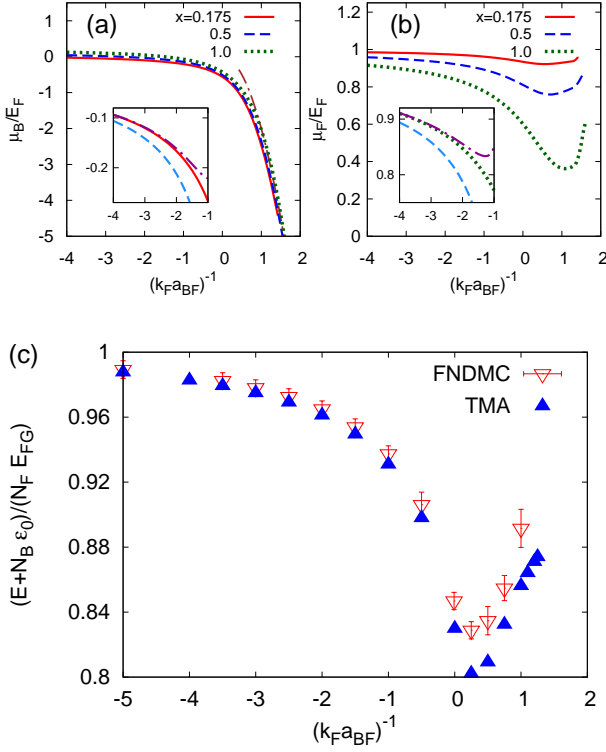


FIG. 2. (a) Bosonic chemical potential μ_B vs. $(k_F a_{BF})^{-1}$ for $m_B = m_F$, $\eta = 3 \times 10^{-3}$, and different values of x . Dashed-dotted line: $-\epsilon_0$. (b) Fermionic chemical potential μ_F for same parameters. Insets: comparison at $a_{BB} = 0$ with 1st (dashed) and 2nd order (dashed-dotted) perturbative results in weak coupling for (a) μ_B at $x = 0.175$ (b) μ_F at $x = 1$. (c) Energy vs. $(k_F a_{BF})^{-1}$ at $x = 0.175$ and $\eta = 3 \times 10^{-3}$, with the binding energy contribution subtracted for $a_{BF} > 0$.

$\epsilon_0 = (2m_r a_{BF}^2)^{-1}$ is the binding energy of the two-body problem, when pairing correlations dominate. In the inset, one can see that our calculated values of μ_B (full line) approach the 2nd order perturbative expression $\mu_B = 2\pi a_{BF} n_F / m_r (1 + 3 \frac{k_F a_{BF}}{2\pi})$ (dashed-dotted line) of Refs. [35, 36]. The fermionic chemical potential μ_F has instead a non-monotonic behavior. For increasing attraction, it first decreases, following the 2nd order perturbative expression $\mu_F = E_F + 2\pi a_{BF} n_B / m_r (1 + 2 \frac{k_F a_{BF}}{\pi})$ in the weak-coupling limit (see inset), and then increases for $(k_F a_{BF})^{-1} \gtrsim 1$, suggesting a repulsion between unpaired fermions and correlated BF pairs, similar to that occurring in the molecular limit.

Figure 2(c) compares the TMA results for the total energy E (normalized to the energy of the free Fermi gas $N_F E_{FG}$, where $E_{FG} = 3E_F/5$) with the FNDMC results for the energy in the superfluid phase for $x = 0.175$ and $\eta = 3 \times 10^{-3}$ [19]. The TMA energy is obtained from the relation $\mu_B = dE/dN_B$ by integrating μ_B from $n_B = 0$ to $n_B = 0.175 n_F$ at fixed n_F , $k_F a_{BB}$, and $k_F a_{BF}$. One sees that the TMA energy follows rather closely the FNDMC data (which are upper bounds to the ground-state energy) even in the fully non-perturbative regime

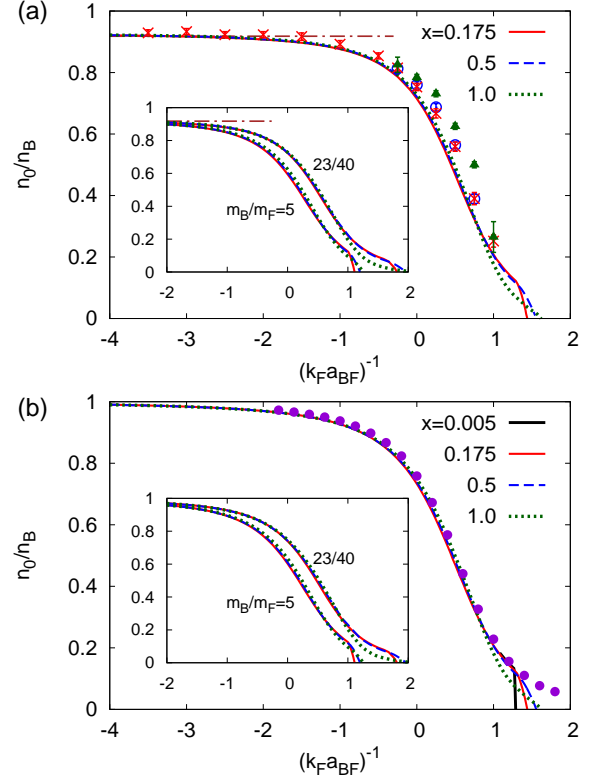


FIG. 3. Condensate fraction vs. $(k_F a_{BF})^{-1}$ for different x . (a) Results for $m_B = m_F$, $\eta = 3 \times 10^{-3}$. Lines: TMA data and (dashed-dotted line) Bogoliubov result $1 - 8/3(\eta/\pi)^{1/2}$. Symbols: QMC data for $x = 0.175$ (crosses), 0.5 (circles), 1 (triangles). (b) Results for $m_B = m_F$, $a_{BB} = 0$. Circles: diag-MC results of Ref. [56] for Z . Insets: results for $m_B/m_F = 5$, $23/40$, with same boson repulsions as in the main graphs.

$|k_F a_{BF}| > 1$. Notice that to emphasize discrepancies, the binding energy contribution $-N_B \epsilon_0$ has been subtracted to both FNDMC and TMA data for $a_{BF} > 0$.

We pass now to discuss the results for the condensate fraction n_0/n_B . A striking feature of Fig. 3(a), reporting n_0/n_B vs. $(k_F a_{BF})^{-1}$ for different x and constant η , is that the curves calculated within TMA at different concentrations collapse on top of each other for most of their graph (specifically, deviations from this universal behavior occur for $n_0/n_B \lesssim 0.2$ where, however, the condensed phase is no longer the ground state, according to the phase diagram of [19]). This occurs not only for $m_B = m_F$, but also for different mass ratios (the inset reports examples for $m_B/m_F = 5, 23/40$, the latter value corresponding to a ^{23}Na - ^{40}K mixture). Our QMC simulations confirm this universality for $x \leq 0.5$, with results very close to TMA. Deviations appear instead for $x = 1$, with larger values of n_0/n_B compared to the results at lower concentrations (or to TMA), with the exception of the point at $(k_F a_{BF})^{-1} = 1$, which has however large error bars due to uncertainties in the QMC extrapolation method at this or larger couplings. Part of this discrepancy could be ascribed to the lack of information on

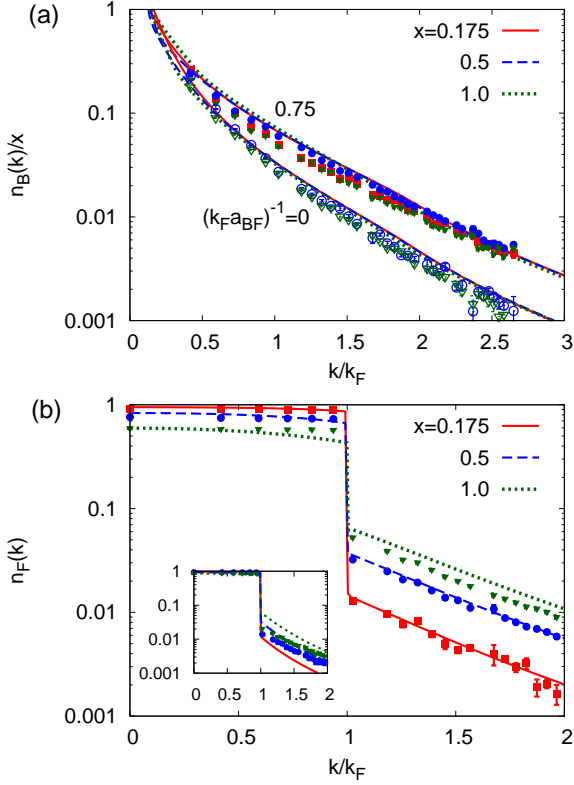


FIG. 4. (a) Bosonic momentum distribution function $n_B(k)$ divided by x vs. k for $m_B = m_F$, $\eta = 3 \times 10^{-3}$, $(k_F a_{BF})^{-1} = 0, 0.75$, and different values of x . Curves: TMA results. Symbols: QMC data for $x = 0.175$ (crosses), 0.5 (circles), 1 (triangles). (b) $n_F(k)$ vs. k for the same parameters as in (a) and $(k_F a_{BF})^{-1} = 0.75$ (main panel) and 0 (inset).

molecular correlations in the nodal surface of Ψ_T , with a consequent increase of n_0/n_B due to an underestimate of the pairing effects, especially at high concentration where interaction effects on the fermions are more important. Moreover, finite-size effects and the use of Jastrow wave functions generally increase n_0 of QMC calculations [46], which we thus consider as an upper bound.

The universality of the condensate fraction just found with both methods for $x \leq 0.5$ prompts us to consider the limit $x \rightarrow 0$, and establish a connection with the problem of a single impurity immersed in a Fermi sea (the ‘polaron problem’ that much attention has received recently in the context of polarized Fermi gases [47–56]). What is the analogous of the condensate fraction for the polaron problem? Consider first the polaron as the $x \rightarrow 0$ limit in a BF mixture. By definition $n_0/n_B = n_B(k=0)/N_B$, then reducing to $n_{\text{imp}}(k=0)$ for $x \rightarrow 0$ (where $n_{\text{imp}}(k)$ is the momentum distribution of a single impurity). Regard now the polaron as the high polarization limit of an imbalanced Fermi gas, and focus on the quasiparticle weight Z at the Fermi momentum $k_{F\downarrow}$ of the minority component (\downarrow). The weight Z determines the height of the Fermi step: $Z = n_{\downarrow}(k_{F\downarrow}^-) - n_{\downarrow}(k_{F\downarrow}^+)$. For vanishingly small concentration $k_{F\downarrow} \rightarrow 0$ and $n_{\downarrow}(k) \rightarrow n_{\text{imp}}(k)$, then

yielding $Z = n_{\text{imp}}(k=0) - n_{\text{imp}}(0^+) = n_{\text{imp}}(k=0)$ for $V \rightarrow \infty$. This is because $n_{\text{imp}}(k \neq 0)$ scales like V^{-1} , since its integral scales like the density of one particle in the volume V . We thus conclude that for $x \rightarrow 0$ the condensate fraction of a BF mixture tends to the polaron quasiparticle weight Z . Figure 3(b) compares then our data for the condensate fraction at different x (and $\eta = 0$ as for the polaron problem) with the diagrammatic Monte Carlo data for the polaron quasiparticle weight Z reported in [56]. We see that the curve at the lowest concentration follows indeed the data for Z for all couplings, until it vanishes almost with a jump at a critical coupling (indicating a real jump for $x = 0^+$). In addition, due to the universality discussed above, also the curves at larger concentrations follow the polaron weight Z , with deviations just in their ending part, where they vanish more gently than at low concentrations. Note further, by comparing Fig. 3(a) and (b), that in the coupling region $(k_F a_{BF})^{-1} \geq 0$ of most interest, the boson repulsion has a minor effect on n_0/n_B . By measuring the condensate fraction in a BF mixture, even at sizable boson concentrations, one would thus obtain Z in a completely different and independent way from the radio-frequency spectroscopy or Rabi oscillations techniques used for imbalanced Fermi mixtures [53, 55].

The universal behavior of n_0/n_B suggests to look for a similar behavior in the whole $n_B(k)$. To this end, we divide $n_B(k)$ by the concentration x , as shown in Fig. 4(a) for both TMA and QMC calculations. The results obtained by the two methods agree well and show that curves and data obtained at different concentrations almost collapse on top of each other. For the fermionic momentum distributions $n_F(k)$ of Fig. 4(b), the agreement between QMC and TMA results is slightly worse. This can be attributed to finite size effects, which are more severe for the fermionic momentum distributions (see the detailed discussion of these effects of Ref. [57]).

In conclusion, we have presented a diagrammatic approach for the condensed phase of a BF mixture which compares well with QMC calculations over an extended range of boson-fermion couplings, including the fully non-perturbative region $|k_F a_{BF}| > 1$. By using both methods, we have found that the condensate fraction and the bosonic momentum distributions are ruled by curves which, in an extended concentration range, are universal with respect to the boson concentration. We have also found an unexpected connection between the condensate fraction in a BF mixture and the quasiparticle weight of the Fermi polaron, unifying in this way features of polarized Fermi gases and BF mixtures.

ACKNOWLEDGMENTS

We acknowledge CINECA and Regione Lombardia, under the LISA initiative, for the availability of high performance computing resources and support. Financial support from the University of Camerino under the

project FAR “CESN” is also acknowledged.

-
- [1] S. Powell, S. Sachdev, and H. P. Buchler, Phys. Rev. B **72**, 024534 (2005).
 - [2] D. B. M. Dickerscheid, D. van Oosten, E. J. Tillema, and H. T. C. Stoof, Phys. Rev. Lett. **94**, 230404 (2005).
 - [3] A. Storozhenko, P. Schuck, T. Suzuki, H. Yabu, and J. Dukelsky, Phys. Rev. A **71**, 063617 (2005).
 - [4] A. V. Avdeenkov, D. C. E. Bortolotti, and J. L. Bohn, Phys. Rev. A **74**, 012709 (2006).
 - [5] L. Pollet, M. Troyer, K. Van Houcke, and S. M. A. Rolambouts, Phys. Rev. Lett. **96**, 190402 (2006).
 - [6] S. Röthel and A. Pelster, Eur. Phys. J. B **59**, 343 (2007).
 - [7] X. Barillier-Pertuisel, S. Pittel, L. Pollet, and P. Schuck, Phys. Rev. A **77**, 012115 (2008).
 - [8] L. Pollet, C. Kollath, U. Schollwöck, and M. Troyer, Phys. Rev. A **77**, 023608 (2008).
 - [9] D. C. E. Bortolotti, A. V. Avdeenkov, and J. L. Bohn, Phys. Rev. A **78**, 063612 (2008).
 - [10] F. M. Marchetti, C. J. M. Mathy, D. A. Huse, and M. M. Parish, Phys. Rev. B **78**, 134517 (2008).
 - [11] T. Watanabe, T. Suzuki, and P. Schuck, Phys. Rev. A **78**, 033601 (2008).
 - [12] E. Fratini and P. Pieri, Phys. Rev. A **81**, 051605(R) (2010).
 - [13] Z.-Q. Yu, S. Zhang and H. Zhai, Phys. Rev. A **83**, 041603(R) (2011).
 - [14] J.-L. Song and F. Zhou, Phys. Rev. A **84**, 013601 (2011).
 - [15] D. Ludwig, S. Floerchinger, S. Moroz, and C. Wetterich, Phys. Rev. A **84**, 033629 (2011).
 - [16] E. Fratini and P. Pieri, Phys. Rev. A **85**, 063618 (2012).
 - [17] A. Yamamoto and T. Hatsuda, Phys. Rev. A **86**, 043627 (2012).
 - [18] P. Anders, P. Werner, M. Troyer, M. Sigrist, and L. Pollet, Phys. Rev. Lett. **109**, 206401 (2012).
 - [19] G. Bertaina, E. Fratini, S. Giorgini, and P. Pieri, Phys. Rev. Lett. **110**, 115303 (2013).
 - [20] E. Fratini and P. Pieri, Phys. Rev. A **88**, 013627 (2013).
 - [21] T. Sogo, P. Schuck, and M. Urban, Phys. Rev. A **88**, 023613 (2013).
 - [22] A. Guidini, G. Bertaina, E. Fratini, and P. Pieri Phys. Rev. A **89**, 023634 (2014).
 - [23] C. Ospelkaus, S. Ospelkaus, L. Humbert, P. Ernst, K. Sengstock, and K. Bongs, Phys. Rev. Lett. **97**, 120402 (2006).
 - [24] S. Ospelkaus, C. Ospelkaus, L. Humbert, K. Sengstock, and K. Bongs, Phys. Rev. Lett. **97**, 120403 (2006).
 - [25] J. J. Zirbel, K.-K. Ni, S. Ospelkaus, J. P. D’Incao, C. E. Wieman, J. Ye, and D. S. Jin, Phys. Rev. Lett. **100**, 143201 (2008).
 - [26] K.-K. Ni, S. Ospelkaus, M. H. G. de Miranda, A. Pe’er, B. Neyenhuis, J. J. Zirbel, S. Kotochigova, P. S. Julienne, D. S. Jin, and J. Ye, Science **322**, 231 (2008).
 - [27] C.-H. Wu, I. Santiago, J. W. Park, P. Ahmadi, and M. W. Zwierlein, Phys. Rev. A **84**, 011601 (2011).
 - [28] C.-H. Wu, J. W. Park, P. Ahmadi, S. Will, and M. W. Zwierlein, Phys. Rev. Lett. **109**, 085301 (2012).
 - [29] J. W. Park, C.-H. Wu, I. Santiago, T. G. Tiecke, S. Will, P. Ahmadi, and M. W. Zwierlein, Phys. Rev. A **85**, 051602 (2012).
 - [30] M.-S. Heo, T. T. Wang, C. A. Christensen, T. M. Rvachov, D. A. Cotta, J.-H. Choi, Y.-R. Lee, W. Ketterle, Phys. Rev. A **86**, 021602 (2012).
 - [31] T. D. Cumby, R. A. Shewmon, M.-G. Hu, J. D. Perreault, and D. S. Jin, Phys. Rev. A **87**, 012703 (2013).
 - [32] R. S. Bloom, M.-G. Hu, T. D. Cumby, and D. S. Jin, Phys. Rev. Lett. **111**, 105301 (2013).
 - [33] C. A. R. Sá de Melo, M. Randeria, and J. R. Engelbrecht Phys. Rev. Lett. **71**, 3202 (1993).
 - [34] P. Pieri and G. C. Strinati, Phys. Rev. B **61**, 15370 (2000).
 - [35] A. P. Albus, S. A. Gardiner, F. Illuminati, and M. Wilkens, Phys. Rev. A **65**, 053607 (2002).
 - [36] L. Viverit and S. Giorgini, Phys. Rev. A **66**, 063604 (2002).
 - [37] A. Perali, P. Pieri, and G. C. Strinati, Phys. Rev. Lett. **93**, 100404 (2004).
 - [38] P. Pieri, L. Pisani, and G. C. Strinati, Phys. Rev. B **72**, 012506 (2005).
 - [39] F. Palestini, A. Perali, P. Pieri, and G. C. Strinati, Phys. Rev. A **82**, 021605 (2010).
 - [40] F. Palestini, P. Pieri, and G. C. Strinati, Phys. Rev. Lett. **108**, 080401 (2012).
 - [41] A simpler T-matrix approach for the condensed phase could be constructed by using Γ in the place of T in the self-energies (3) and (7). This approach is however correct only to first order in the weak-coupling limit of the BF interaction, while our T-matrix approach is consistent to second order. We have also explicitly verified that this alternative T-matrix approach yields quite different (and rather unphysical) results for the condensate fraction compared to Monte Carlo calculations and the present T-matrix approach.
 - [42] See, e.g., Sec. 9 of A. Fetter and J. D. Walecka, *Quantum Theory of Many-Particle Systems* (Mc-Graw Hill, New York, 1971).
 - [43] N. M. Hugenholtz and D. Pines, Phys. Rev. **116**, 489 (1959).
 - [44] P. J. Reynolds, D. M. Ceperley, B. J. Alder, and W. A. Lester, J. Chem. Phys. **77**, 5593 (1982).
 - [45] M. Casula, C. Attaccalite, and S. Sorella, J. Chem. Phys. **121**, 7110 (2004).
 - [46] L. Reatto, Phys. Rev. **183**, 334 (1969).
 - [47] N. V. Prokof’ev and B. V. Svistunov, Phys. Rev. B **77**, 125101 (2008).
 - [48] M. Veillette, E. G. Moon, A. Lamacraft, L. Radzihovsky, S. Sachdev, and D. E. Sheehy, Phys. Rev. A **78**, 033614 (2008).
 - [49] P. Massignan, G. M. Bruun, and H. T. C. Stoof, Phys. Rev. A **78**, 031602(R) (2008).
 - [50] C. Mora and F. Chevy, Phys. Rev. A **80**, 033607 (2009).
 - [51] M. Punk, P. T. Dumitrescu, and W. Zwerger, Phys. Rev. A **80**, 053605 (2009).
 - [52] R. Combescot, S. Giraud, and X. Leyronas, Europhys. Lett **88**, 60007 (2009).
 - [53] A. Schirotzek, C.-H. Wu, A. Sommer, and M. W. Zwierlein, Phys. Rev. Lett. **102**, 230402 (2009).

- [54] C. J. M. Mathy, M. M. Parish, and D. A. Huse, Phys. Rev. Lett. **106**, 166404 (2011).
- [55] C. Kohstall, M. Zaccanti, M. Jag, A. Trenkwalder, P. Massignan, G. M. Bruun, F. Schreck, and R. Grimm, Nature **485**, 615 (2012).
- [56] J. Vlietinck, J. Ryckebusch, and K. Van Houcke, Phys. Rev. B **87**, 115133 (2013).
- [57] M. Holzmann, B. Bernu, C. Pierleoni, J. McMinis, D. M. Ceperley, V. Olevano, and L. Delle Site, Phys. Rev. Lett. **107**, 110402 (2011).